ISSN No:-2456-2165

Energy Spectrum of Converters and Positron Range Estimation in PET Simulation For 511-keV Photons

Muhammad Afzaal Sadaqat[1] and Dr. Ijaz Ahmed[2]
[1,2]Riphah International University. I-14 Hajj Complex,
Islamabad, Pakistan

Abstract:- The purpose of this study was to observe the energy distribution of incident 511-keV photons produced as a result of annihilation effect $e^-+e^+ \rightarrow \gamma+\gamma$ in three different electrodes (of aluminum, glass, and Bakelite). The transmission, absorption, and reflection of particles for 511-keV photons were examined using a thin or thick layer of electrodes. Moreover, the manner in which the energy spectrum of a single electrode changes with its thickness was explored. The positron range of the positron emission tomography (PET) radioisotopes is responsible for the production of high-quality images in (PET) imaging reconstruction. As a result, the ranges and kinetic energies of positrons from three radioisotopes (F^{18}, O^{15}, I^{124}) were calculated in this study using the Geant4 application for tomographic emission (GATE) simulation package. Notably, the ranges thereof were determined via their energies.Finally, the simulated ranges and kinetic energy values were compared with the literature values revealing a 0.5% difference.

Keywords:- *Annihilation effect, Positron Emission Tomography (PET), Imaging reconstruction, Radioisotopes.*

I. INTRODUCTION

The growing interest in positron emission tomography (PET) in medical imaging reconstruction has facilitated development of techniques allowing healthcare professionals to see inside a patient's body without directly looking at a camera or performing an open surgery and forming qualitative images. PET is currently the most preferred imaging method in clinical research. Short-lived radionuclides are endowed with subjective tissue that emits positrons at a time based on their respective half-lives in this procedure. This positron travels some distance (~mm) in a tissue before it annihilates with an electron to produce two back-to-back 511-keV photons traveling at 180° to each other. In this regard, an activity distribution in a tissue can be created by aggregating several interaction events [1]. PET is noninvasive imaging technique, used in tomography for small animals, that involves good time resolution, a potentially high spatial resolution, and low cost [2].

Herein, we used Geant4 to simulate the energy distribution of 511-keV photons for various electrode materials. The Geant4 simulation package was designed specifically for the passage of charged particles through matter. Ionization and excitation of gas molecules result in energy losses in charged particles, and the type of interaction determines the cross-section of the energy loss. The total energy loss is depicted in the following equation [3].

$$-1/\rho dE/dx|_{col}=CN_A/A[\ln\pi^2\gamma^3(m_ec^2)2/I^2 - a] \quad (1)$$

Here, 'ρ' is the density of the particles, 'dE/dx' is the energy loss, and 'C' is a constant expressed in MeV/cm^2. For electrons a=2.9 and positrons a=3.6. 'I' represents the intensity, 'm_e' represents the mass of electrons, and 'A' is the mass number of the absorbing material.

In the second part of this study, we used GATE to estimate the ranges and kinetic energies of positrons of F^{18}, O^{15}, and I^{124} radionuclides in PET simulations for the case of 511-keV photons.

II. ENERGY DISTRIBUTION OF 511-KEV PHOTONS

Geant4 was used to examine the energy spectrum formed upon incidence 511-keV photons on various electrodes. Fig. 1 depicts an image of the energy deposited on three different electrodes as a result of this simulation. Because of the photoelectric effect, the rate of energy deposition abruptly decreases at 340-keV photon energy. The low electrical resistivity of aluminum ($10^{-8}\Omega$-cm) implies a lower resistance offered to incoming photons than of glass and Bakelite. As a result, there existed more events in which energy was deposited takes place at the electrode.

ISSN No:-2456-2165

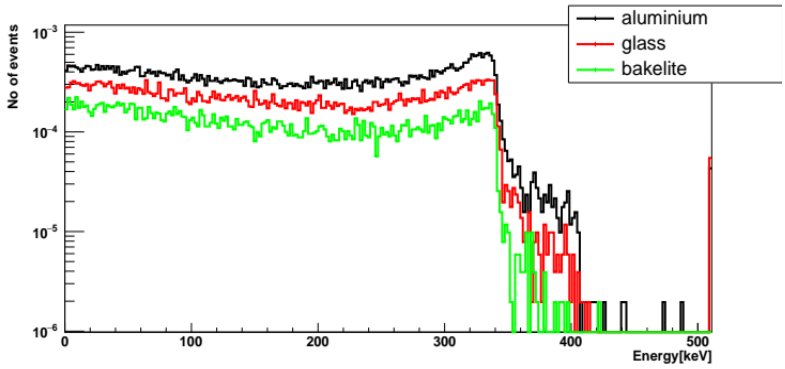

Fig 1: Energy deposited at absorber dN/ Kinetic Energy at Exit dN/dE

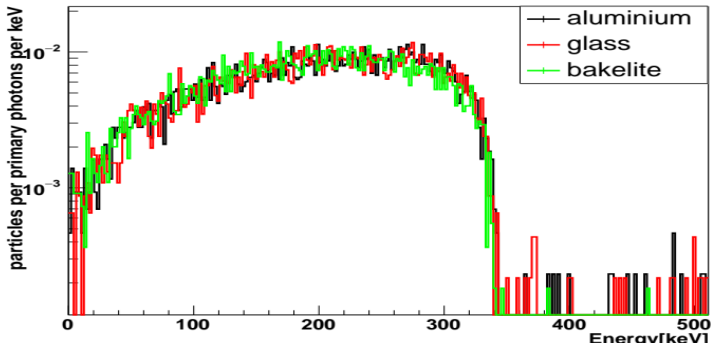

Fig 2: Transmitted Compton Electrons Kinetic

Fig. 2 depicts the kinetic energy of the transmitted Compton electron at the exit point. Electron extraction from an electrode reveals that there is no electrical resistive effect on the energy of the transmitted Compton electrons. Moreover, energy fluctuations up to 240-keV occur for transmitted Compton photons 9 (Fig. 3).

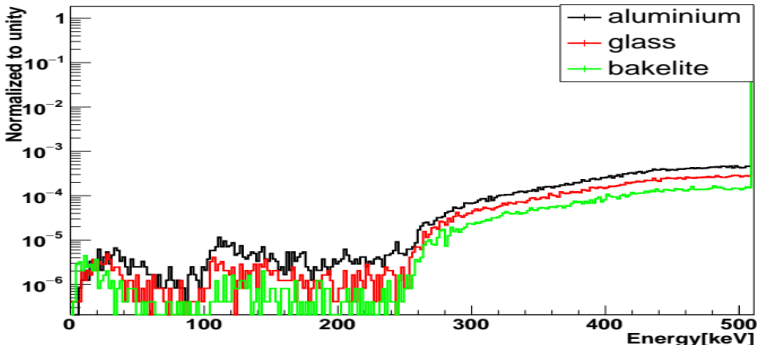

Fig 3: Transmitted Compton Photon Kinetic Energy at Exit dN/dE

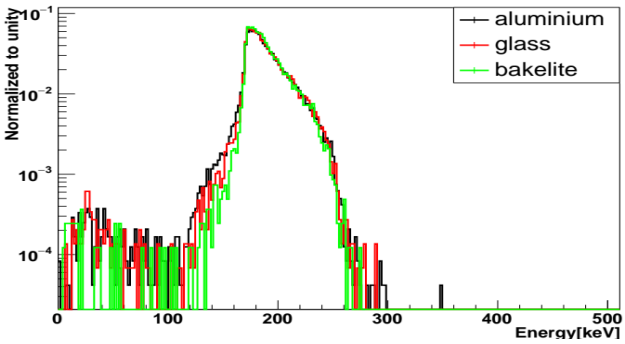

Fig 4: Reflected Compton Photon Kinetic Energy at Exit dN/De

ISSN No:-2456-2165

Because photons are produced at energies lower than this, by the photoelectric effect or multiple scattering [1]. Photons are scattered at 90° at 240-keV energy, but the probability rate increases at higher energy. The maximum probability of Compton photons can be seen at a very high energy (~ 511 keV).

Because of the thinness of the electrode material (2 mm), one out of every ten events in which incident photons with energies of 180 keV leave the crystal without interacting and are thus scattered on the electrode entrance window is shown in Fig. 4. Backscattered particles are thought to be very important in the simulation of single-layer crystals with sufficient dimensions and their scattering properties [4]. The energy deposition and energy of Compton electrons and Compton photons for the aluminum electrode are depicted in Fig. 5. Because, electrons produce intense ionization in the gas gap and cause avalanches at higher energies, the probability rate decreases with energy; there are very few events at higher energy.

Fig. 6 depicts the kinetic energy of the transmitted Compton electrons and Compton photons for the Bakelite electrode. Because of the photoelectric effect, the probability of events for Compton electrons decreases at 340-keV photon energy. The curve fluctuates up to photon energy of 240-keV for transmitted Compton photons. Photons with energies less than 240-keV are produced as a result of the photoelectric effect or multiple scattering. Photons are scattered at 90º at 240 keV, resulting in a longer path through the solid material before reaching the gas volume [1].

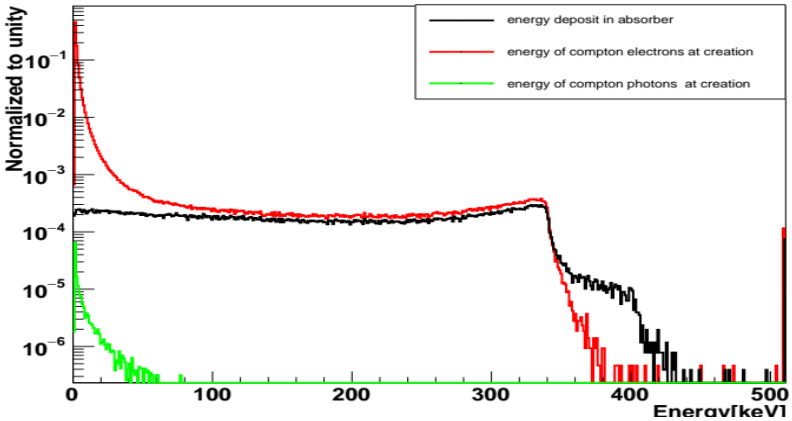

Fig 5: Energy spectrum of Compton electrons Compton photons absorbed and at creation of aluminum electrode.

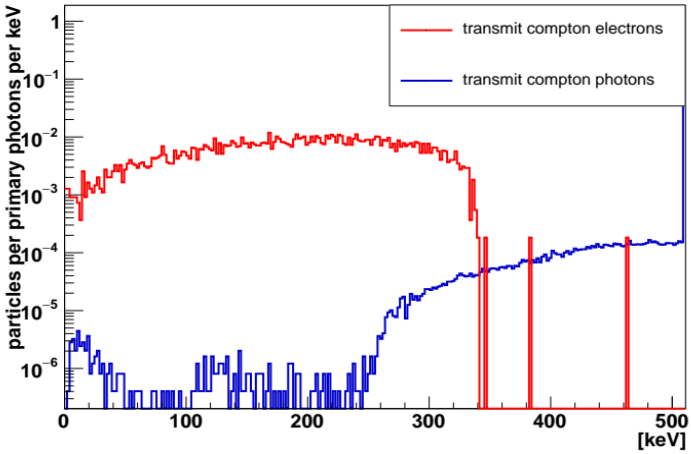

Fig 6: Transmitted Compton electrons and Compton photons kinetic energy at exit.

However, owing to the thinness of the glass electrode material (~2mm), 70% of the incident photons leave the crystal without interacting and may enter the glass electrode window (Fig. 7). The reflected Compton electrons have a low speed and high ionizing ability; therefore, the rate of reflection is extremely low [4].

ISSN No:-2456-2165

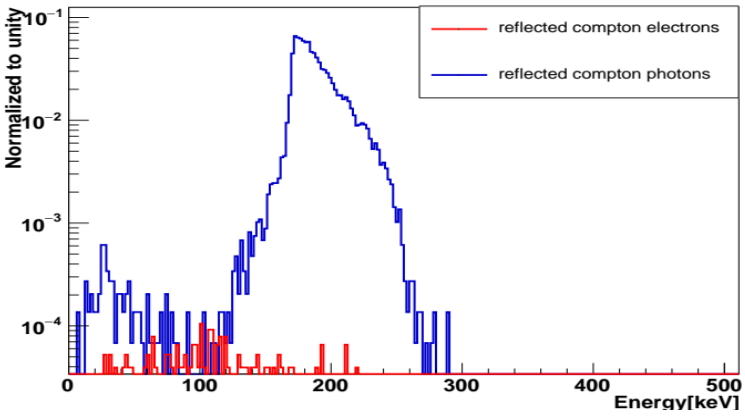

Fig 7: Reflected Compton electrons and Compton photons kinetic energy at exit

III. VARIATION OF ENERGY DISTRIBUTION WITH ELECTRODE THICKNESS

Further, we checked the alteration of the energy spectrum curves at the end of this process by changing the thickness of the electrode (aluminum). Upon variation of the thickness, the probability of transmitted Compton electrons, energy deposited at the absorber, and energy of the Compton electrons at creation remains constant (Fig 8 a,c,d)). Notably, only the probability of transmission of the Compton photons increases with electrode thickness (Fig 8 b). As a result, the greater is the probability of transmission of Compton photons, the higher is the electrode material thickness.

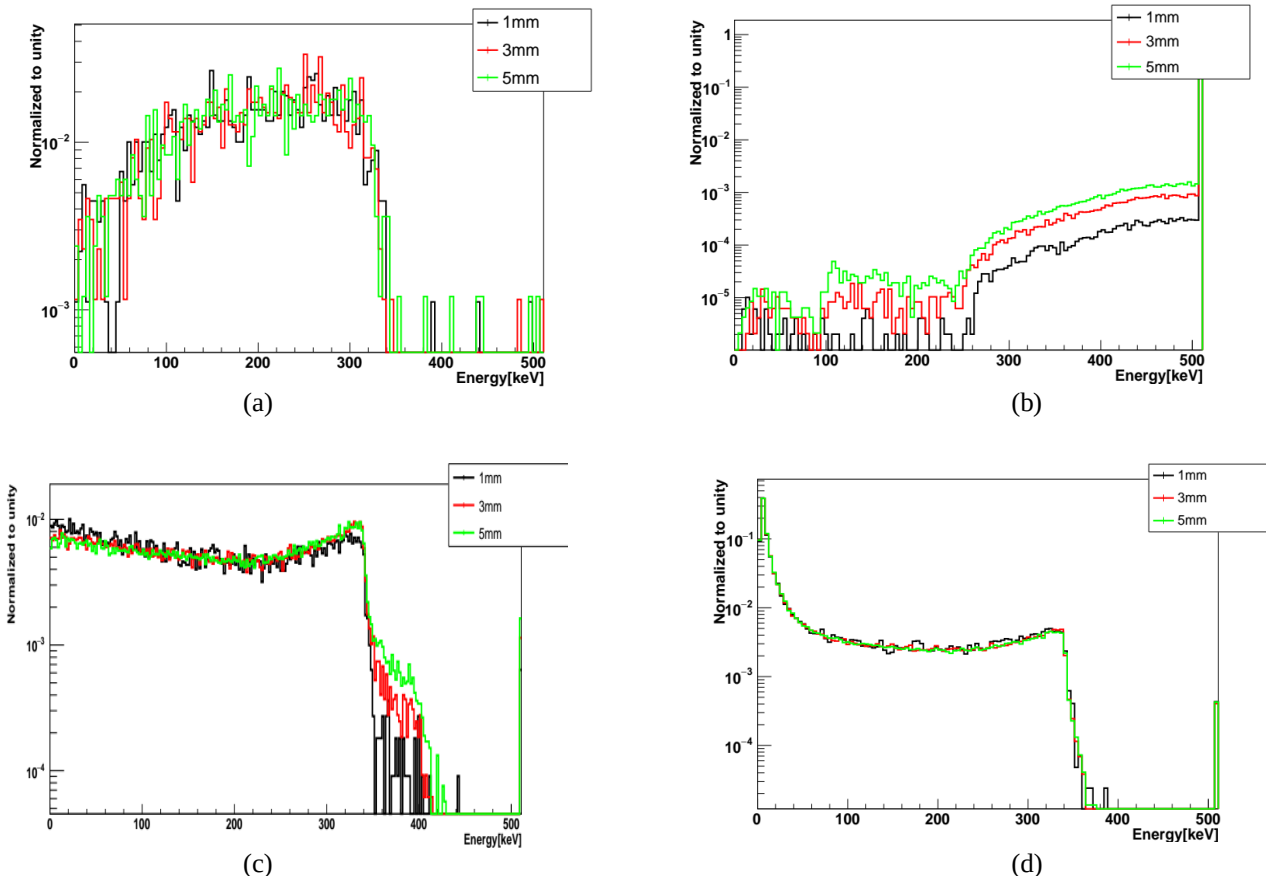

Fig. 8: Variation of energy spectrum with electrode thickness (a) transmitted Compton electrons (b) transmitted Compton photons (c) energy deposited at absorber (d) Compton electrons energy at creation

ISSN No:-2456-2165

IV. ESTIMATION OF POSITRON RANGE AND KINETIC ENERGY

The positron travels a certain distance in the tissue before annihilating into two photons. This is the distance between the point of emission and the point of annihilation in Euclidean space and represents a significant advancement in PET imaging blurring. Blurred images are considerably improved during imaging reconstruction through accurate estimation of the positron range. We estimated the positron range for three commonly used PET radioisotopes F^{18}, O^{15}, and I^{125} using the GATE simulation toolkit. These radioisotopes are found in a variety of biological media including striated muscle, brain, soft bone, water, lung, adipose tissue, cortical bone, and skin [6]. We compared the GATE simulation results to those found in the literature (Table 1 and 2) and our findings are observed to be consistent with those of experiments.In this case, the majority of the simulations conducted previously had a mean and maximum range discrepancy of less than 20%. Based on these measurements, we conclude that a more accurate simulation setup is required particularly to disengage the positronium formation effect in the positron range. The spectra of positron range and kinetic energy are shown in Fig. 8 and Fig. 9 respectively. Three columns exist in the output text: X(mm), Y(mm), and Z(mm). Each set of points represents the position vector of the range values as well as their respective coordinate systems. By accurately calculating the norm value of each data set using formula (2), one can estimate the mean and maximum value of the positron's range.

$$r = \sqrt{x^2+y^2+z^2} \quad (2)$$

where, r represents the range, moreover, x, y, and z are the position vectors of the range along the x, y, and z-axis respectively. Notably, their energies determined their ranges, and fluorine's positrons were found to be short-range ones (~2mm) whereas, iodine's positronswere found to be long-range ones (~10mm). The spatial resolution of the image can be improved by using short half-lived radionuclides. As a result of its short half-life, short positron range, and better spatial resolution, fluorine is the most frequently used radioisotope in the PET imaging [5].

F^{18} has half life $t_{1/2}$= 110 min and disintegrates into O^{18} by β^+ (96.9%) and electron capture (3.1%). The emitted positrons have R_{max}= 2.3 mm and R_{mean}= 0.64 mm with the corresponding energies E_{max}= 0.63 MeV and E_{mean}= 0.25 MeV. O^{15} disintegrates into N^{15} with a half-life of $t_{1/2}$= 2 min by β^+ (99.9%) and electron capture (0.1%). The range of its positron emission is R_{max}= 8.4 mm and R_{mean}= 3.0 mm and its corresponding energies are E_{max}= 1.73 MeV and E_{mean}= 0.73 MeV. Similarly, I^{124} decays under a long half-life of 100h into Te^{124} by β^+ (22.7%) and electron capture (77.3%). Its positron range is calculated as R_{max}= 10.2 mm and R_{mean}= 4.4 mm and its corresponding energies are E_{max}= 2.13 MeV and 0.97 MeV.

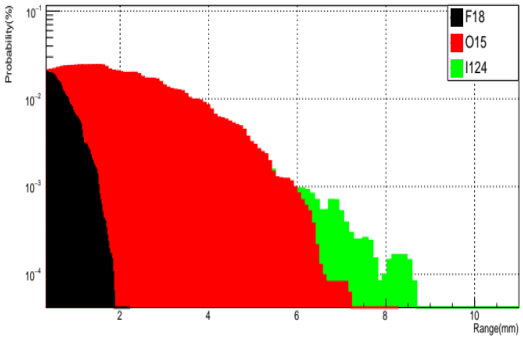

Fig. 9: Positron range (mm)

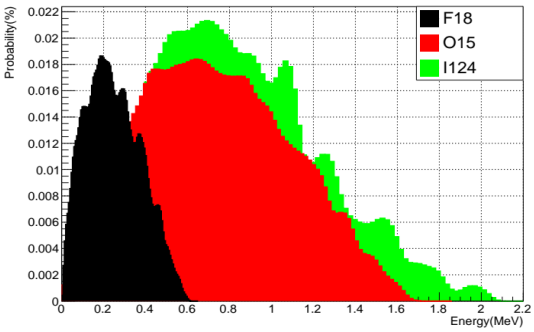

Fig. 10: Positron kinetic energy (MeV)

	R_{max}		< R > : Most Probable Range	
	# Simulation	**# Data**	**# Simulation**	**# Data**
F^{18}	2.04 mm	2.3 mm	0.43 mm	0.64 mm
O^{15}	7.2 mm	8.4 mm	4.01 mm	3.0 mm
I^{124}	9.16 mm	10.2 mm	2.34 mm	4.44 mm

Table 1: Positron range (mm)

	E_{max}		< E > : Most Probable Energy	
	# Simulation	**# Data**	**# Simulation**	**# Data**
F^{18}	0.60 MeV	0.63 MeV	0.21 MeV	0.25 MeV
O^{15}	1.60 MeV	1.73 MeV	0.42 MeV	0.73 MeV
I^{124}	2.10 MeV	2.13 MeV	0.51 MeV	0.97 MeV

Table 2: Positron kinetic energy (MeV)

V. CONCLUSION

In this study, in the case of incident 511-keV photons, we observed the manner in which energy is distributed for three electrode materials: aluminum, glass, and Bakelite. Compton scattering is thought to be the primary phenomenon governing interaction with fluctuations of the energy distribution of Compton photons and Compton electrons occuring at photon energies of 340 keV. In addition, we investigated the variation in the energy spectrum of a single electrode (aluminum) as its thickness varies. Finally, we extracted certain GATE results that show the ranges and kinetic energies of positrons for different radionuclides F^{18}, O^{15}, and I^{124}. The ranges and kinetic energy values that we simulated for the F^{18}, O^{15}, and I^{124} radioisotopes resemble the literature values, indicating that our simulation model is valid.

REFERENCES

[1.] Lippmann, C., Vincke, H., & Riegler, W. (2009). Simulation of RPC performance for 511 keV photon detection. Nuclear Instruments and Methods in Physics Research Section A: Accelerators, Spectrometers, Detectors, and Associated Equipment,602(3), 735-739.

[2.] Weizheng, Z., Ming, S., Cheng, L., Hongfang, C., Yongjie, S., & Tianxiang, C. (2014). Monte Carlo Simulation of RPC-based PET with GEANT4.arXiv preprint arXiv:1402.4544.

[3.] B. Rossi. High Energy Particles. Prentice-Hall, Inc., Englewood Cliffs, NJ, 1952.

[4.] Santin, G., Strul, D., Lazaro, D., Simon, L., Krieguer, M., Martins, M. V., ... & Morel, C. (2003). GATE: A Geant4-based simulation platform for PET and SPECT integrating movement and time management. IEEE Transactions on nuclear science, 50(5), 1516-1521.

[5.] Conti, M., & Eriksson, L. (2016). Physics of pure and non-pure positron emitters for PET: a review and a discussion. EJNMMI Physics,3(1), 1-17.

[6.] Cal-González, J., Herraiz, J. L., España, S., Corzo, P. G., Vaquero, J. J., Desco, M., & Udias, J. M. (2013). Positron range estimations with PeneloPET. Physics in Medicine & Biology, 58(15), 5127.